Ferroelectrics

ISSN: 0015-0193 (Print) 1563-5112 (Online) Journal homepage: https://www.tandfonline.com/loi/gfer20

# The Influence of Acceptor Doping on the Structure and Electrical Properties of Sol-Gel Derived $BiFeO_3$ Thin Films

K. Brinkman, T. Iijima, K. Nishida, T. Katoda & H. Funakubo

**To cite this article:** K. Brinkman, T. Iijima, K. Nishida, T. Katoda & H. Funakubo (2007) The Influence of Acceptor Doping on the Structure and Electrical Properties of Sol-Gel Derived $BiFeO_3$ Thin Films, Ferroelectrics, 357:1, 35-40, DOI: 10.1080/00150190701527597

**To link to this article:** https://doi.org/10.1080/00150190701527597

*Ferroelectrics*, 357:35–40, 2007

ISSN: 0015-0193 print / 1563-5112 online
DOI: 10.1080/00150190701527597

Taylor & Francis
Taylor & Francis Group

# The Influence of Acceptor Doping on the Structure and Electrical Properties of Sol-Gel Derived $BiFeO_3$ Thin Films

K. BRINKMAN,[1,*] T. IIJIMA,[1] K. NISHIDA,[2] T. KATODA,[2] AND H. FUNAKUBO[3]

[1] Research Center for Hydrogen Industrial Use and Storage, AIST, Tsukuba Central 5, Tsukuba 305-8565, Japan
[2] Kochi University of Technology, Kamishi, Kochi 782-8502, Japan
[3]Department of Innovative Engineered Materials, Tokyo Institute of Technology, 4259 Nagatsuta, Midori-ku, Yokohama 226-8502, Japan

*Bismuth Ferrite (BFO) films doped with strontium resulting in a nominal composition of $Bi_{1-x}Sr_xFe_1O_3$ ($x = 0$–$0.15$) were fabricated using a sol-gel process on $Pt/TiO_2/SiO_2/Si$ substrates by rapid thermal annealed in air at 700°C. A decrease in the grain size (from 1 μm to 90 nm) with increasing Sr concentration from 0 to 15% was observed, coupled with the degradation of columnar grain growth. X-ray diffraction and raman scattering showed evidence of a structural change from rhombohedral to pseudocubic with increasing Sr concentration. Leakage measurements revealed that films with Sr acceptor doping showed increased leakage compared to pure BFO, however the film leakage did not increase with increasing acceptor concentration due to microstructural modifications.*

**Keywords** Thin film; sol-gel; raman scattering

## Introduction

Bismuth Ferrite ($BiFeO_3$) thin films have been a recent topic of interest as multiferroic materials which combine the two properties of ferromagnetism, and ferroelectricity with important potential applications in the development of new magnetoelectric devices [1, 2]. Recently numerous researchers have explored chemical deposition methods for thin film fabrication, taking advantage of the method's facility for introducing low levels of dopant elements in order to tailor film properties [3–6]. At the current stage of materials development, there are significant questions remaining concerning the impact of processing, and the effects of dopants on the structure and properties of BFO thin films.

The addition of dopants has been shown to impact the electrical properties of BFO films through (i) structural modifications such as a reduction in crystal anisotropy as well as (ii) through modification of the defect chemistry in the system which determines oxygen vacancy concentration and resulting film conduction. In pure BFO, the often observed large

Received September 3, 2006; accepted September 7, 2006.
*Corresponding author. E-mail: kyle.brinkman@a3.epfl.ch

leakage current has been attributed to the multivalent Fe ion leading to oxygen vacancies [7]. Transition metal doping with isovalent and aliovalent ions has been investigated with preferential substitution at the B site using Cr [3], Mn and Nb [5], Ti and Ni [8]. It was found in these studies that that low levels of doping up to ∼5% did not significantly affect the film structure resulting in a nominally pseudocubic or rhombohedral like structure. Donor doping with Nb or Ti ion and isovalent doping with Cr generally improved the leakage current density and ferroelectric properties, while acceptor doping with Ni and isovalent doping with Mn increased the leakage current and proved harmful for ferroelectric properties. In contrast to B site doping where no structural changes were observed, a recent publication by Uchida investigated the effects of isovalant doping of the A site with La and Nd [6] showing a degradation in crystal anisotropy value and curie temperature of doped BFO films resulting in smaller remnant polarization values. The effect of doping on the microstructure and resulting electrical properties has not been significantly studied.

In order to further investigate fundamental properties of this material system, the current study focus on the impact of A site acceptor Sr doping at levels from 0 to mol 15% on the structure and properties of BFO thin films. Due to the ionic radius of $Sr^{+2}$ (1.12 A) compared to the $Bi^{+3}$ ion (1.2 A), "A" site substitution is expected. In the following, it is shown that Sr doping affects the crystal structure, microstructure and electrical properties of BFO thin films.

## Experimental

BFO films were prepared using chemical solution deposition technique using bismuth acetate, iron acetylacetonate and strontium acetylacetonate in an acetic acid/water solution (ratio acetic acid:$H_2O$ = 2:1). The 0.5 M solution was heated to ∼80°C while stirring for 1 hour to promote dissolution of the precursor, followed by stirring at room temperature for 1 day before film deposition. The solution composition was synthesized based on the assumption of A site substitution resulting in the chemical formula $Bi_{1-x}Sr_xFe_1O_3$ ($x = 0$, 0.02, 0.05 and 0.15). Films were deposited on $Pt/TiO_2/SiO_2/Si$ substrates by spin coating at 3000 rpm for 30 seconds, followed by a drying step at 100°C for 2 min and pyrolysis at 350°C for 2 min. Rapid thermal annealing of the films to 700°C for 3 min duration in air was performed after each 4 layers of the deposition/pyrolysis procedure resulting in ∼1 $\mu$m thick films after 20 layers (5 RTA annealing steps). Top electrodes of Pt were sputter deposited with a diameter of ∼500 $\mu$m to provide contact for subsequent electrical measurement. The crystal structure of films was examined by X-ray diffraction (XRD) on a Philips X-pert diffractometer and the microstructure was determined by scanning electron microscopy (SEM) Hitachi. The leakage current was measured using a Hewlett Packard 4140B electrometer 0.1 V step and a waiting time of 3 s for each step. Raman spectroscopy was performed using a Renishaw System 1000 with an $Ar^+$ laser of 514.5 nm used as the excitation source. The beam spot size was ∼1 micron and measuring time was 60 seconds. Estimates of the raman scattering modes from mass and bond strength methods were made assuming the R3c space group of BFO [9].

## Results and Discussion

The X-ray diffraction patterns (XRD) of 1 micron thick BFO thin films with 0, 2, 5 and 15% Sr doping are shown in Fig. 1(a). The films exhibited a random orientation and no secondary phases could be detected within the uncertainty of the XRD measurements.

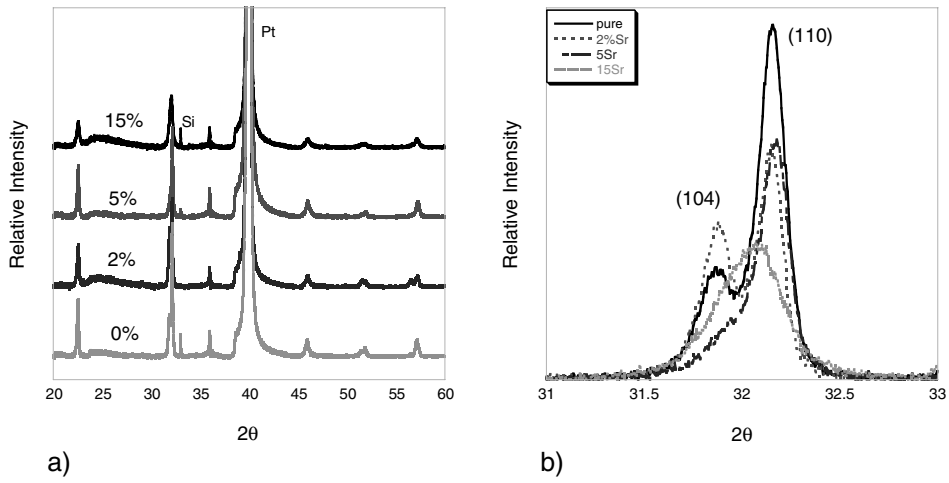


**Figure 1.** (a) X-ray spectra of 1 micron BFO films with 0, 2, 5 and 15% Sr additions (b) X- ray scan of the (104)/(110) spectral region. (See Color Plate II)

Figure 1(b) displays a close up view of the 31 to 33 two-theta region comprising the (104) and (110) diffraction peaks of rhombohedral BFO (JCPDS X-ray database 86-1518). It is seen that there is a change in crystal structure with increasing Sr concentration. Pure BFO and low 2% doping level of Sr exhibit distinct (104) and (110) peaks, however further addition of Sr up to 5% leads to the appearance of only a single peak in the spectral region corresponding to a loss of anisotropy and a change to a pseudocubic phase. Further additions of Sr up to 15% also show only one diffraction peak in this range. The relative broadness of the 110 peak with 15% Sr addition is believed to be the result of the small grain size (below 100 nm).

An examination of the film microstructure using SEM is shown in Fig. 2 indicating that low levels of Sr doping (2%) did not drastically affect the surface morphology of the films, resulting in 500 nm to 1 $\mu$m grain size features grown in a columnar fashion from the Pt bottom electrode. Additions of 5% Sr reduced the grain size from the micron range down to 150 nm, thus disturbing the columnar growth mechanism. Additions of 15% Sr resulted in a grain size below $\sim$90 nm, with no evidence of columnar growth. These samples displayed distinct horizontal layers filled with pores and voids. Chung [5] reported a decrease in grain size with increasing donor doping of Nb. It was proposed that donor doping decreased the concentration of oxygen vacancies thus slowing down oxygen diffusion and limiting grain growth. The results of this work show a decrease in grain size with increasing concentration of acceptor doping; since the oxygen vacancy concentration is expected to increase the grain growth in our samples should not be inhibited by oxygen diffusion. A possible mechanism for the observed fine grain structures is the formation of SrO during the pyrolysis step, whose cubic crystal structure may facilitate the nucleation of the pseudocubic perovskite phase during the structural evolution from an amorphous to the final crystalline state. Another possible reason for the altered film nucleation and growth could be the increased the organic content of the Sr doped sols resulting from higher concentration of acetylacetonate ligands present in the Sr chemical precursor.

Thin film raman measurements of pure BFO and Sr doped samples from 2, 5 and 15% are presented in Fig. 3. It is expected that the peak shift of the A site in BFO should be below 100 $cm^{-1}$ [10] while modes corresponding to the B site would occur at higher

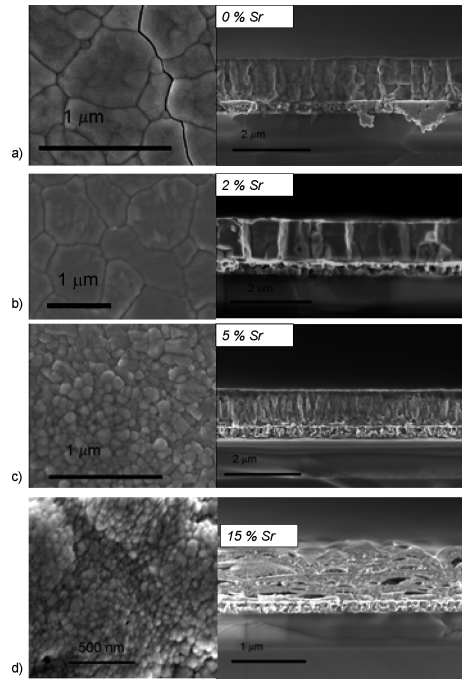


**Figure 2.** SEM determined microstructure: plane view and cross section (a) pure BFO (b) 2% Sr (c) 5% Sr (d) 15% Sr.

energies (higher $cm^{-1}$). Figure 3(b) shows a close up of the low energy spectral region. It is seen that a peak at 75 $cm^{-1}$ shifts to lower energy region with increasing Sr addition, while modes above 100 $cm^{-1}$ are unaffected. This result confirms the basic assumption that due to ionic radius arguments, $Sr^{2+}$ is substituted for $Bi^{3+}$ on the A site.

The observed downward shift is in contrast to that expected from considerations of the atomic mass of Sr (87 amu) as compared to Bi (208 amu). The substitution of the lighter Sr element would be expected to display higher frequency vibrations leading to an upwards shift of the raman peak. This is indicated by the line labeled "Mass Effect" in Fig. 3(c). Consideration of the bond strength estimated from bond-valence parameters [11] resulted in the line labeled "Force Constant" in Fig. 3(c), which predicts a peak shift to lower energies

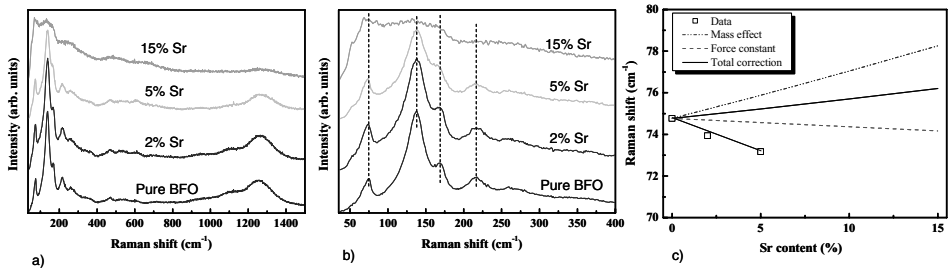


**Figure 3.** (a) Un-polarized raman spectra: Full view of BFO films with 0, 2, 5, 15% Sr additions (b) Enlarged view of the A site (below 100 $cm^{-1}$) and B site (above 100 $cm^{-1}$) peak shift regions (c) estimated versus measured peak shift. (See Color Plate III)

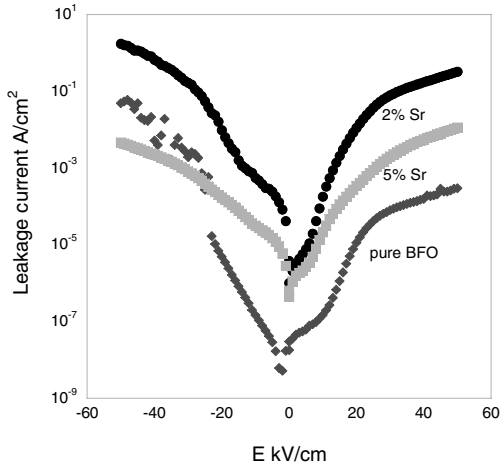


**Figure 4.** J-E leakage characteristics of pure and Sr doped BFO films measured at room temperature. (See Color Plate IV)

with Sr addition. However, the total estimated peak shift, labeled "Total Correction" (mass effect minus force constant) still shows significant difference with the experimental data. We believe this discrepancy is a result of an inaccurate estimation of the bond strength. The covalency of the Bi─O bond as compared to the ionic Sr─O bond has been recently confirmed in theoretical studies [12] pointing to the disruption of the strong covalent Bi─O bonding by the weaker Sr─O ionic bond as a possible source of the raman peak shift in the present case.

The room temperature leakage characteristics of pure BFO, 2 and 5% Sr doped samples are presented in Fig. 4. In pure BFO and 2% Sr doped samples there is an asymmetry observed when switching from positive to negative fields revealing the presence of an interface effect. In general, the addition of Sr increased the leakage current as would be expected as a result of an acceptor doping increase of the oxygen vacancy concentration. At room temperature the leakage current density at 40 kV/cm was $1.5 \times 10^{-4}$, $1.7 \times 10^{-1}$ and $5.6 \times 10^{-3}$ A/cm$^2$ for 0, 2 and 5% Sr doped samples. The leakage behavior is not a simple function of Sr concentration: at low field levels up to 10 kV/cm, the leakage of 2 and 5% Sr doped samples is similar, however the sample with 2% Sr shows an increase of leakage by over 2 orders of magnitude at higher fields than the 5% Sr doped sample. That is to say, the sample with an ostensibly greater oxygen vacancy concentration displays less film leakage. This behavior can be explained with reference to the Sr doping induced changes in microstructure presented in Fig. 3. Films doped with 5% Sr are assumed to have a higher concentration of oxygen vacancies and would display higher film leakage if the film microstructure was comparable. However, the decrease in grain size and disruption of columnar grain growth with high levels of Sr doping led to an increase in grain/grain boundary interfaces in the bulk of the film which did not provide a clear pathway for conduction.

## Conclusion

The structure and electrical properties of BFO films prepared using sol-gel methods were found to depend on the concentration of Sr additions. Substitution of Sr on the A site

was confirmed by raman scattering leading to a structural change from rhombohedral to pseudocubic and a decrease in grain size with increasing Sr content. Film leakage was not a simple function of Sr concentration highlighting the importance of film microstructure on the electrical properties of BFO thin films.

## Acknowledgments

We acknowledge the JSPS for funding and support. Dr. Hiroshi Naganuma (Tokyo University of Science) is gratefully acknowledged for assistance with leakage measurements.

## References

1. J. Wang, J. Neaton, H. Zheng, V. Nagarajan, S. Ogale, B. Liu, D. Viehland, V. Vaithyanathan, D. Schlom, U. Waghmare, N. Spaldin, K. Rabe, M. Wuttig, and R. Ramesh, *Science* **299**, 171 (2003).
2. K. Yun, M. Noda, and M. Okuyama, *Appl. Phys. Lett.* **83**, 3981 (2003).
3. J. Kim, S. Kim, W. Kim, A. Bhalla, and R. Guo, *Appl. Phys. Lett.* **88**, 132901 (2006).
4. S. Iakovlev, C. Solterbeck, M. Kuhnke, and M. Es-Souni, *J. Appl. Phys.* **97**, 094901 (2005).
5. C. Chung, J. Lin, and J. Wu, *Appl. Phys. Lett.* **88**, 242909 (2006).
6. H. Uchida, R. Ueno, H. Funakubo, and S. Koda, *J. Appl. Phys.* **100**, 014106 (2006).
7. W. Zhu and Z. Ye, *Ceramics International* **30**, 1435 (2004).
8. X. Qi, J. Dho, R. Tomov, M. Blamire, and J. MacManus-Driscoll, *Applied Physics Letters* **86**, 062903 (2005).
9. C. Michel, J. Moreau, G. Achenbach, R. Gerson, and W. James, *Solid State Communications* **7**, 701 (1969).
10. A. Litvinchuk, M. Iliev, V. Popov, and M. Gospodinov, *J. Phys.: Condens. Matter.* **16**, 809 (2004).
11. I. Brown and D. Altermatt, *Acta Cryst.* B**41**, 244 (1985).
12. T. Shishidou, N. Mikamo, Y. Uratani, F. Ishii, and T. Oguchi, *J. Phys.: Condens. Matter* **16**, S5677 (2004).